Landslide susceptibility assessment in mountainous and tropical scarce-data regions using remote sensing data: a case study in the Colombian Andes.

Diana Ruiz-Vásquez[1], Edier Aristizábal[2]

1. Department of Geology, EAFIT University; 2. Environmental and Geoscience Department, National University of Colombia

Abstract

Landslides triggered by rainfall are one of the most frequent causes for natural disasters in the tropical and mountainous countries, such as Colombia. However landslide susceptibility assessments are often limited due to the scarcity of reliable observations and available information, particularly in remote high-mountain regions. Although Colombia is a tropical and mountainous terrains dominated by landslide prone region, it has little availability of data for landslide susceptibility assessment. This study presents the application of a logistic regression model to assess landslide susceptibility in the La Liboariana catchment. It is a basin on a tropical inaccessible terrain in northern Colombian Andes, where on May 18th, 2015, more than 40 landslides and an associated flash flood and debris flow afterwards killed 104 inhabitants. The applied approach is based on free access remote sensing tools to complete and obtain the missing landslide causative factors. To select key factors related to landslide occurrence the prediction and successes performance of the susceptibility maps for each combination of landslide causative factors was estimated using the Receiver Operating Characteristics (ROC). The results show that only three factors gave the best predicting accuracy. All the factors were obtained by free remote sensing tools, indicating they can provide enough information to achieve a successful approach to landslide susceptibility assessment in complex terrains as the study area. This suggests that the proposed approach could be implemented in several tropical regions with similar characteristics based only in free access information.

Keywords

GIS; logistic regression; remote sensing; landslide susceptibility; tropical basin; Colombia

1 Introduction

Landslides are among the most deadly natural hazard and cause large economic losses all over the world each year (Alexander, 2005; Nadim, Kjekstad, Peduzzi, Herold, & Jaedicke, 2006; Schuster, 1996; Schuster & Highland, 2001). In fact, around 5 percent of the total global population lived in landslide prone areas (Dilley, Chen, Deichmann, Lerner-Lam, & Arnold, 2005), and in countries

such as the United States, Japan, Italy, and India economic losses are estimated over $1 billion per year (Schuster & Fleming, 1986). It has been estimated that between 2004 and 2010 a number of 32.322 people lost their lives as a result of nonseismic landsliding (Petley, 2012).

Rainfall is the most common cause of landslides (Guzzetti, Peruccacci, Rossi, & Stark, 2007; Iverson, 2000; Zêzere, Trigo, & Trigo, 2005) and has been responsible for the highest number of casualties, the 89,6 % of worldwide landslide fatalities were a result of landslides triggered by rainfall (Petley, 2008). Based on the EM-DAT database from OFDA/CRED, between 2005 and 2014 an world annual average of 914 deaths caused by landslides triggered by rainfall were reported (Guha-Sapir, Hoyois, & Below, 2016).

Landslides triggered by rainfall are one of the most frequent causes for natural disasters in the tropical and mountainous countries of the Circum-Pacific region (Schuster, Salcedo, & Valenzuela, 2002; Sepúlveda & Petley, 2015; Varnes, 1981). Colombia, located in the northern corner of South America, is characterized by tropical conditions and mountainous terrains. The most important urban centers are located in the highlands and valleys of the Andes Mountains. Because of this natural conditions Colombia has a long history of landslide disasters. A debris flow on November 13, 1985 devastated the city of Armero killing around 22.000 people and economical losses over $339 million (Garcia, 1988; Mileti, Bolton, Fernandez, & Updike, 1991; Voight, 1990). In the city of Medellin on September 27, 1987 a mudslide with a volume of 20,000 m^3 destroyed more than 80 houses and killed around 500 people (Tokuhiro, 1999). Recently on April 1, 2017 a total of 130 mm of torrential rains triggered several landslides in the mountainous terrains of the southern Colombian Andes causing a flash flood and debris flow along the Mocoa, Sangoyaco and Mulato rivers that destroyed 17 neighborhoods of the city of Mocoa, which were built along the river banks. At least 314 people were killed and a further 106 were missing (Cruz Roja Colombiana, 2017).

However landslide impacts assessments are often limited due to the scarcity of reliable observations, particularly in remote high-mountain regions, such as the Colombian mountains. Data availability is one of the most important factors for analysis, assessment and modeling of landslides triggered by rainfall. The areas affected by landslides are often remote and difficult to access. For this reason the development of regional landslide susceptibility analysis has proven difficult in the places where it is most needed (De Graff, Romesburg, Ahmad, & McCalpin, 2012). Due to this lack of data in many regions, remote sensing data may be used to landslide susceptibility analysis in developing countries. Although such data sometimes might not have the accuracy and precision of

directly measured data, appropriate methodologies and satellite data could be used to overcome the limitations and produce adequate landslide susceptibility maps.

Landslide susceptibility assessment is critical for planning, sustainable development and risk mitigation because provide information on the likelihood of landslides occurring in an area given the local terrain conditions (Brabb, 1984). Although, there are several methodologies to assess landslide susceptibility, they can be divided into qualitative or knowledge driven methods and quantitative or data driven methods (Aleotti & Chowdhury, 1999). Knowledge driven methods are based entirely on the judgment of the earth scientist, and the baseline data for zoning comes directly from field visits (Cardinali et al., 2002; van Westen, Soeters, & Sijmons, 2000). A main limitation of qualitative method is that the accuracy depends on the knowledge of the experts. Data driven methods are subdivided into deterministic and statistically based methods (Baum, Savage, & Godt, 2008; Pack, 1998). While deterministic methods assess slope failures using the factor of safety at large scales (Montgomery & Dietrich, 1994) and required detail information and parameters, the statistical methods evaluate the relationship between landslide and causative factor to predict the occurrence probabilities through the use of GIS tools, reducing the subjectivity and biases in the process of weighting landslide causative factors. The widely used statistical methods are bivariate (Aleotti & Chowdhury, 1999; Lee, 2005; Süzen & Doyuran, 2004), multivariate (Carrara, 1983; Gorsevski, P.V.; Gessler, P.;Foltz, 2000; Lee & Pradhan, 2007), and neural networks (Ermini, Catani, & Casagli, 2005; Lee, Ryu, Won, & Park, 2004). Logistic Regression (LR) is the multivariate statistical analysis method most widely used (Ayalew & Yamagishi, 2005; Bai et al., 2010; Brenning, 2005; Chevalier, Medina, Hürlimann, & Bateman, 2013; Greco, Sorriso-Valvo, & Catalano, 2007; Lee & Pradhan, 2007). LR is independent on data distribution and can incorporate into the analysis a variety of data sets such as continuous, categorical, and binary data. However the selection of landslide causal factors are significant to logistic regression methods (Lee & Talib, 2005). Irrelevant independent variables should be removed, and include into the analysis only optimal causative factors (Lee & Talib, 2005; Pradhan & Lee, 2010).

This case study aims to contribute to the knowledge by applying a methodology to assess landslide susceptibility in a data-scarce study area in the Colombian Andes, where on May 18th, 2015, dozens of landslides were triggered by a rainstorm, leading to a major debris flow and flash flood, causing a total of 104 deaths and economic losses not estimated yet. The study uses Satellite DEM, Google Earth, othophotos and aerial photography. To select the positive causative factors related to landslide occurrence and the validation of the model the area under the ROC curve was applied.

2 Study Area

The Liboriana catchment is located in the northern side of the Western Cordillera in the Colombian Andes, about 500 km northwest of Bogota City (Fig. 1). It lies between latitudes 5º55'30"N - 6º1'0"N and longitudes 75º58'W - 76º6'W, and covers an area of nearly 59 km^2. Two populated areas extend along the central and lower portion of the river valley, named La Margarita village and Salgar town, which have a population of about 8.820 inhabitants.

The catchment has a tropical humid climate with a mean annual temperature of 22 °C. The maximum temperature occurs between February and April, while the minimum between October and November. The precipitation regime is dominated by high variability at both inter-annual and inter-seasonal scales. The mean annual rainfall is 3073 mm; and the monthly rainfall distributions show evident seasonal patterns with two rainy seasons, with rainfall peaks in May and October (Poveda, 2004; Poveda et al., 2005).

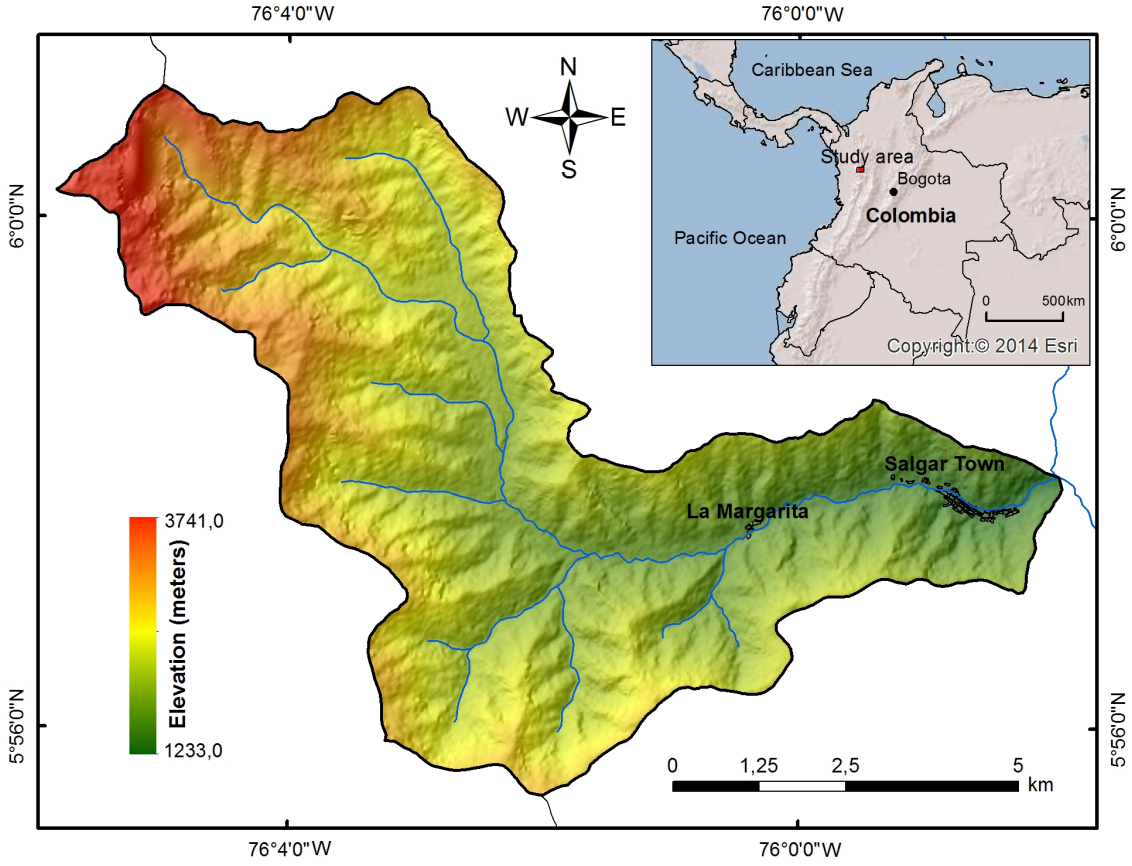

Fig. 1 Location of the Liboriana River basin on the mountainous terrain in Western Cordillera of the Colombian Andes.

The geomorphology of the catchment exhibits in the upper part a mountain region with a rugged morphology, narrow valleys, and very steep forested hillslopes. The elevation varies from 1233 to 3741 m a.s.l. with a mean of 2487 m a.s.l. The area with slope gradients exceeding 30° accounts for the 67% of the total area. The upper part of the catchment consists of deep forests, while in the middle and lower zones grasslands and coffee plantations have already substituted forest.

The geological area that comprises the La Liboriana catchment is composed predominately by a Cretaceous sedimentary rock formation (shales, limolites, sandstones, cherts and conglomerates with some intercalations) and an intrusive Miocene body (Calle, González, de la Peña, Escorce, & Durango, 1980; Calle & Salinas, 1984). These rocks have been severely weathered in situ under the humid tropical climate forming residual soils and saprolite.

3 The May 18th, 2015 rainstorm

On 18 May 2015 heavy rains in the northern Colombian Andes caused a MORLE-type landslide (multiple-occurrence regional landslide event) (Crozier, 2005) in the La Liboriana catchment. The great majority of the individual landslides constituting this MORLE event displaced all the regolith, leaving rock exposed. But because of the steep slope of the terrain, surficial rockslides also occurred. A huge amount of water and solid material went down to the main channel of the river and caused a flash flood and a debris flow sweeping away everything in its paths, including La Margarita village and the lowest areas of Salgar Town. Authorities confirmed 104 deaths, 62 people were injured and 1440 were directly affected. At least 66 houses and 6 local bridges were completely destroyed by the flash flood and debris flow. The disaster is the fourth deadliest weather-related disaster in Colombia's recorded history.

Reports from the SIATA weather radar (Early Warning System of the city of Medellin and the Aburrá Valley, in spanish) indicate that between 10 pm on May 17th and 2 am on May 18th a rain cell on the west side of the catchment, place known as Cerro Plateado, caused a very intense precipitation in about 30% of the total area of the basin (~20 km^2). During this four-hour period the total accumulated rainfall was 100 mm. Other minor rains occurred until 7 pm on May 18th, for a total of 160 mm of rain that fell in the upper part of the basin in a 24 hour period.

Google Earth provided a free and open post-event satellite imagery, which permitted to obtain the event landslide inventory and the flash flood path and area occupied by the debris flow (Fig. 2).

Around 160 shallow landslides were triggered by the May 18th, 2015 rainstorm, but in the La Liboriana catchment a total of 50 landslides were identified.

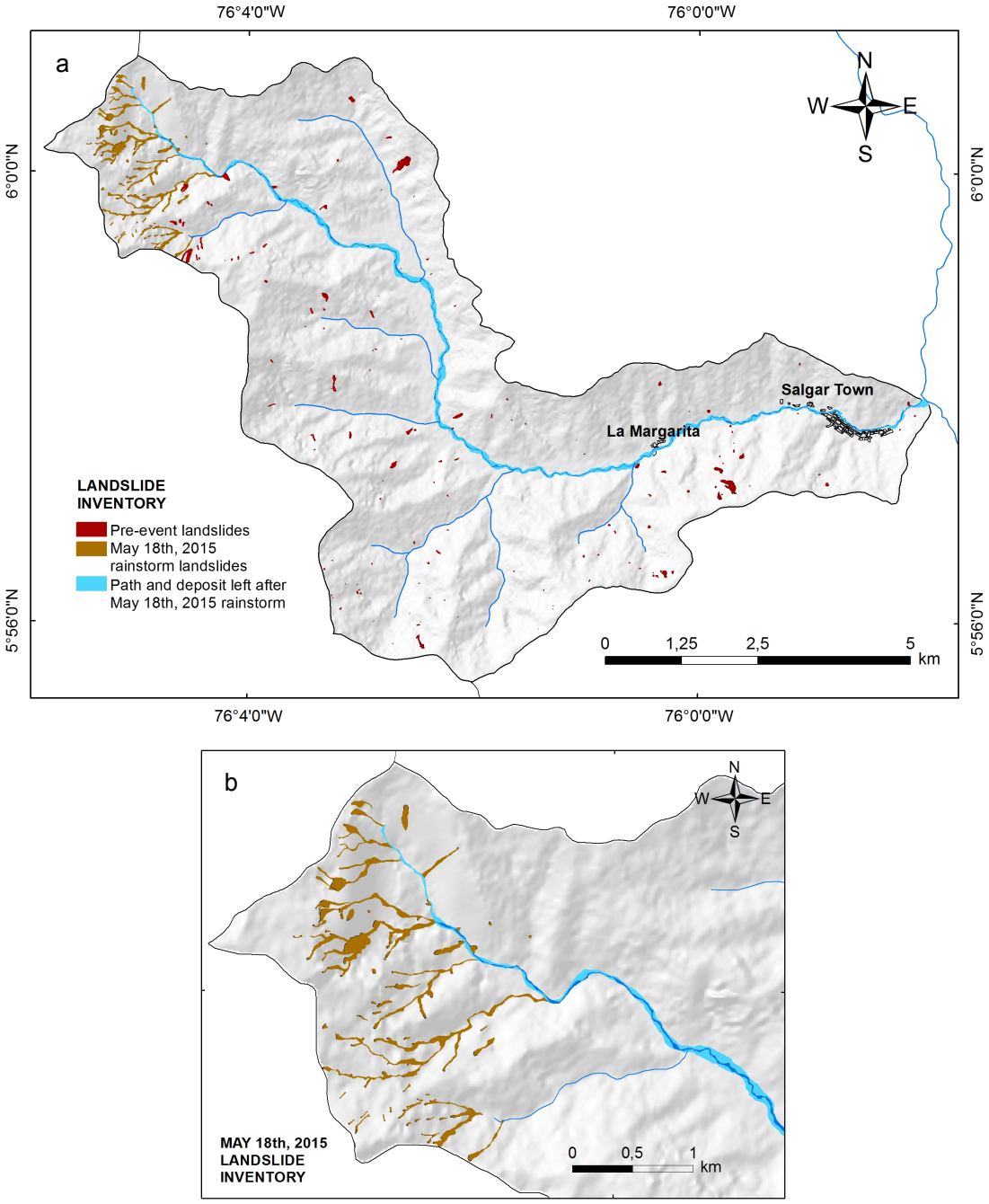

Fig. 2 Landslide inventory map. (a) complete inventory obtained by the multi-temporal analysis, (b) detail of May 18th, 2015 rainstorm landslides.

4 Methodology

A wide range of quantitative methodologies are used to landslide susceptibility assessment (Aleotti & Chowdhury, 1999; Chacón, Irigaray, Fernández, & El Hamdouni, 2006; Fell et al., 2008; Guzzetti, Carrara, Cardinali, & Reichenbach, 1999; Soeters & van Westen, 1996). Statistical methods estimate landslide probabilities based on correlation analysis between causative factors and historical landslide occurrence. Logistic Regression (LR) is one of the most frequently used multivariate statistical analysis models to predict landslide occurrence at medium and regional scales (Ayalew & Yamagishi, 2005; Brenning, 2005; Lee & Pradhan, 2007). LR estimates the relationship between a dependent variable, measured with dichotomous values such as 0 and 1, and a set of independent terrain variables. The advantage of LR is that the predictor factors does not compulsorily require a normal distribution data, and may be either categorical or non-categorical, or any combination of both types (Atkinson & Massari, 1998). Quantitatively, the dependency relationship between landslide occurrence and the independent variables can be expressed as:

$$P(y) = 1/(1 + e^{-z}) \quad (1)$$

where $P(y)$ is the estimated spatial probability of landslide occurrence and ranges from 0 to 1. And z is the following linear combination of the independent factors:

$$z = b_0 + b_1x_1 + b_2x_2 + b_3x_3 + b_nx_n \quad (2)$$

where b_0 is the intercept of the model given in the LR output, the bi values (i=1, 2, 3, …, n) are the regression coefficients, i.e. variable weights; and the xi values (i=1, 2, 3, …, n) are the independent factors. The final model is then a LR based on the independent variables of the occurrence of landslides (presence or absence).

The LR algorithm was applied for landslide susceptibility assessment of the La Liboriana catchment using the IBM Statistical Package for Social Science (SPSS) for five different causative factor combinations (Table 1).

In order to validate the accuracy and prediction capability of the models and to select the best susceptibility model, different validation methods were applied. The most common validation methods in landslide studies are thresholds independent approaches, especially the Receiver Operating Characteristic (ROC) analysis (Fawcett, 2006, Chung & Fabbri, 2003). ROC analysis is based on the Confusion Matrix, in which actual classes, called positives and negative class label,

according to landslide inventory databases, are compares with the predictive classes, called true and false class labels, produced by the model. (Fawcett, 2006). Figure 3 shows the four possible outcomes of the Confusion Matrix. An advantage of ROC analysis is that several statistic have been defined for evaluating models performance and prediction. During the performance and prediction evaluation the hit rate (TPR), false alarm rate (FPR) and odds ratio (OR) were calculated and used for a quantitative comparison.

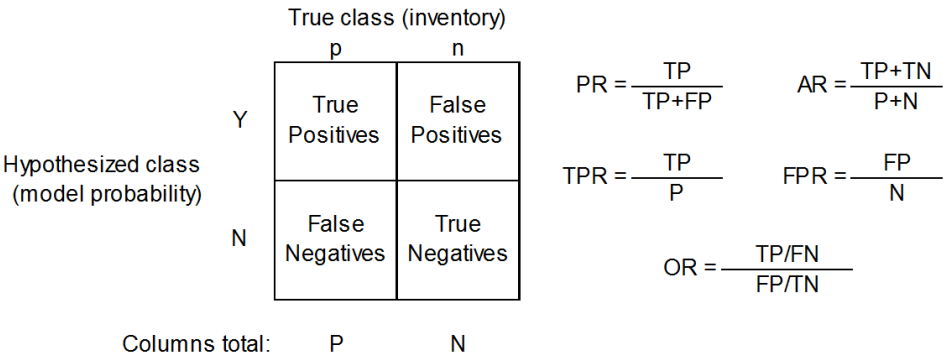

Fig. 3 ROC analysis confusion matrix.

The area under the ROC-curve (AUCROC) is a useful indicator to validate the success and prediction performance of the model. AUC is between 0 and 1, a higher value indicates a higher prediction success or prediction rate, whereas a value near 0,5 means the prediction is not better that a random guess (Chung and Fabbri, 2003).

Table 1 Combination of causative factors of the five different susceptibility models to apply LR.

Models	Included factors	Missing factors
M1	Aspect, land cover, curvature, slope, TWI	
M2	Land cover, curvature, slope, TWI	Aspect
M3	Aspect, land cover, slope, TWI	Curvature
M4	Aspect, land cover, curvature, slope	TWI
M5	Aspect, land cover, slope	Curvature, TWI

Additionally to this analysis, the distance to perfect classification (r) (Cepeda, Chávez, & Cruz Martínez, 2010; Kirschbaum et al., 2015), and the degree of fit (D.F.) (Fernández, Irigaray, El Hamdouni, & Chacón, 2003) were calculated using the following equations:

$$r = \sqrt{(FPR^2 + (1 - TPR)^2)} \quad (3)$$

$$D.F. = \frac{Z_i/S_i}{\sum Z_i/S_i} \quad (4)$$

where Z_i is the area occupied by the rupture zones in the i class of susceptibility and S_i is the area if the i class of susceptibility.

Landslide inventory

Landslide inventories are the first and most important step in landslide susceptibility analysis by statistical methods (Chung & Fabbri, 2003; De Graff et al., 2012; Guzzetti et al., 2012; Kavzoglu, Kutlug Sahin, & Colkesen, 2015; Lin et al., 2013). In this study, landslide locations were determined using the 2015-updated Google Earth imagery, an open access 1:10.000 scale orthophoto from the period 2010-2012, and aerial photography from 1998 and 1999. As a result, a total of 259 landslides were collected (Fig. 2). All landslides cover an area of 0,56 km^2, and accounts for approximately 0,95% of the catchment. Which 33% of them correspond to landslides triggered by the 16 May 2015 rainstorm, and the 67% correspond to multitemporal landslides with no time occurrence specification that occurred previous to the 16 May 2015 event.

Considering the cross validation method proposed by Chung & Fabbri (2003), the landslide inventory data was split into three groups: (i) the training dataset which correspond to 80% of the pre-event and multitemporal landslide inventory to be used for building the LR model (167 landslides); (ii) the spatial validation dataset which correspond to 20% of randomly selected landslides of the pre-event and multitemporal landslide inventory to be used for the spatial validation process (42 landslides); and (iii) the event-based landslide inventory of 50 landslides associated to the May 18th, 2015 storm, which were used to carry out a temporal validation of the landslide susceptibility map.

In addition to landslide areas, non-landslide areas are required to form the dichotomous variable to apply the LR (Kavzoglu et al., 2015). In this study, non-landslide points were determined by randomly choosing the same amount of pixels from the areas with no record of landslides.

Several mapping strategies are used to elaborate a landslide inventory map (Hussin et al., 2016). Spatial location of landslides are represented by points which correspond in raster-based maps to the centroid of the entire landslide or the scarp area (Brenning, 2005; Galli, Ardizzone, Cardinali, Guzzetti, & Reichenbach, 2008; Thiery, Malet, Sterlacchini, Puissant, & Maquaire, 2007; Van Den Eeckhaut et al., 2006), polygons which correspond to all the pixels within the entire landslide body or the scarp area (Ayalew & Yamagishi, 2005; Chung & Fabbri, 2003; van Westen et al., 2000), and lines which correspond to the pixels of the upper edge of the landslide scarp area (Clerici, Perego, Tellini, & Vescovi, 2002; Donati & Turrini, 2002). Several studies have indicated the scarp as the

best sampling strategy to landslide susceptibility assessment (Poli & Sterlacchini, 2007; Simon, Crozier, de Roiste, & Rafek, 2013; Yilmaz, 2010). In this study was adopted the scarp of landslide to represent pre-failure conditions, excluding both the transport and the deposition zones of existing landslides.

Landslide causative factors

The selection of the relevant causative factors is a fundamental step in the landslide susceptibility analysis because improve the prediction accuracy (Costanzo et al., 2012; Kavzoglu et al., 2015; Lee and Telebi, 2005; van Westen et al., 2000). In general, they must have a certain affinity with the dependent variable, must be fairly represented all over the study area, have to be measurable and non-redundant (Ayalew & Yamagishi, 2005). In this study, based on data availability and topographic, hydrological and geological catchment conditions, a total of 5 landslide predictor variables were initially used. They were divided into morphometric and environmental factors.

Morphometric factors. The available topographic maps (1:25.000 and 1:10.000 scales) only cover about 25% of the eastern-most part of the study area. To obtain the topographic features, a free access Digital Elevation Model (DEM) was obtained from the Alaska Satellite Facility program (ASF-DAAC, 2015) with a spatial resolution of 12,5 m. This DEM was used to derive aspect, curvature, slope gradient, and topographic wetness index (TWI) using ArcGIS 10.2 software (Fig. 3). All these factors are related to landslides to a different degree. The relationship between aspect and landslide occurrence has been widely studied (Ayalew, Yamagishi, Marui, & Kanno, 2005; Bai et al., 2010; Pourghasemi, Mohammady, & Pradhan, 2012). Slope aspect is related to sunlight exposure and soil moisture condition of hillslopes (Greco et al., 2007) (Fig 4a). Down-slope and across-slope curvature values were calculated and crossed to obtain total curvature according to Ayalew & Yamagishi (2002) (Fig 4b). Profile curvature influences the driving and resisting stresses within a landslide in the direction of motion and controls the change of velocity of landslide flowing down the slope, whereas the plan curvature controls the convergence of landslide material and water in the direction of the landslide motion. Slope angle is usually defined as the crucial landslide-conditioning factor because it controls the shear forces acting on hillslopes. However, its relationship is not always proportional, the maximum relative frequency of landslides usually corresponds to medium slope angles (Fig. 4c) (Greco et al., 2007). Finally, Topographical Wetness Index (TWI) is an hydrological factor frequently used in landslide studies (Moore, Grayson, & Ladson, 1991; Pawluszek & Borkowski, 2016; Pourghasemi et al., 2012) (Fig. 4d). It is a function of the slope and the upstream contributing area per unit width orthogonal to the flow direction.

Environmental factors. In a tropical landslide-dominated zone such as the La Liboriana River Basin, land use is normally found to be associated with landslide occurrence (Pawluszek & Borkowski, 2016; Tazik, Jahantab, Bakhtiari, Rezaei, & Alavipanah, 2014). The available data on land use was only a 1:100.000 map, very large-scale for the purposes of this study. So the used data was obtained mainly using Google Earth imagery and supported by the 2010-2012 orthophoto to make a detailed map. The resulting layer in the GIS includes six categorical values (Fig. 4e): agricultural land, bare land, forest, grassland, urban area and water body.

Although lithology is one of the essential conditioning factors in most of the landslide susceptibility analysis, in the La Liboriana catchment about 90% of the total area correspond to plutonic igneous rocks (Calle et al., 1980; Calle & Salinas, 1984). This geological homogeneity indicates that lithology does not explain the landslide distribution and spatial location.

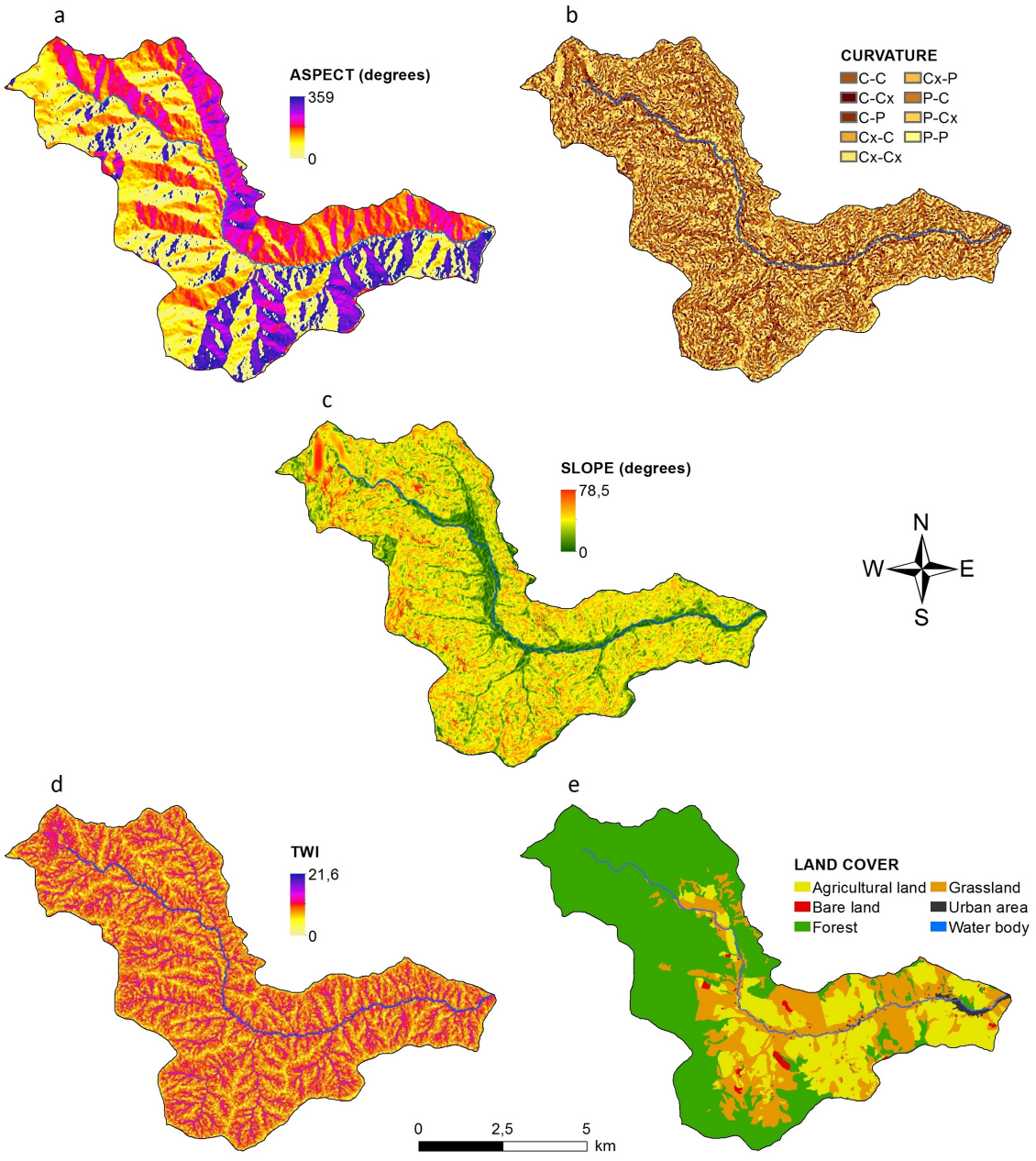

Fig. 4 Liboriana River basin land cover and morphological settings. Each map is one of the five factors included in the LR model. (a) aspect, (b) curvature, (c) slope and (d) TWI, were obtained as derivate variables of the high resolution DEM; and (e) land cover, using mainly Google Earth imagery.

5 Results

Pre-event landslide inventory was divided into landslide group and non-landslide group for each terrain and classed into intervals to plot the frequency distributions for the different causative

factors (Fig. 5). It could be seen that slope, aspect and land cover are the factors that have a tighter relationship with landslide occurrence, since there is a most significant difference between landslide and non-landslide curves.

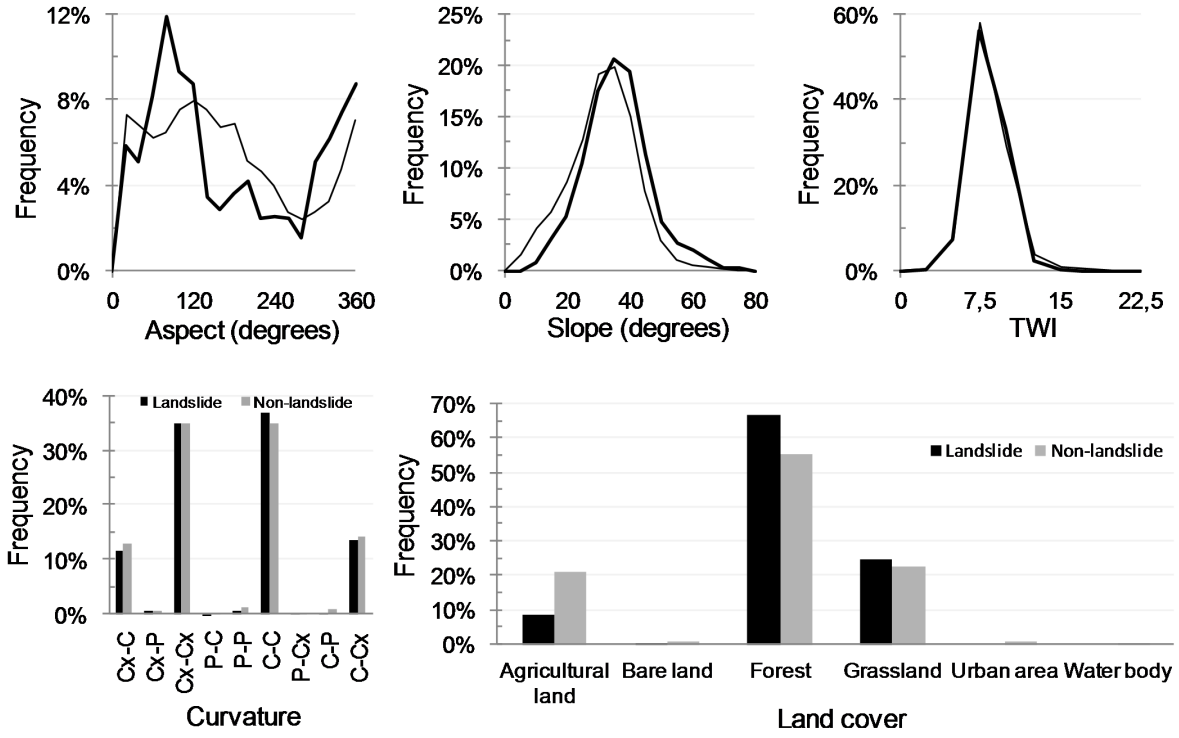

Fig. 5 Frequency distribution of landslide and non-landslide groups in each variable. Topographical Wetness Index (TWI).

According to the slope aspect the frequency of landslides increase on east-facing and north-facing slopes. The correlation analysis between slope angle and landslide occurrence has a normal distribution. Gentle slopes have a low landslide frequency, increasing up to reach at maximum value around 40°, and followed by a decrease of landslide frequency. Steep natural slopes resulting from outcropping bedrock usually are not susceptible to shallow landslides. Regarding the land cover, the results show the majority of landslides falls into the category of forest and grassland cover areas.

For the Topographical Wetness Index (TWI) and curvature, it is not noted a difference between landslide and non-landslide groups. For the case of curvature landslide usually occurred in horizontal and vertical concave or convex slopes. Ad for the TWI factor, landslide frequency normally occurred around values of 8.

LR was applied for the five susceptibility models shown in Table 1. The regression coefficients of the predictor were used to create the landslide susceptibility map for the five susceptibility models. Quantitative validation was conducted by comparing the five susceptibility maps with the landslide spatial distribution inventory, the landslide inventory group 1 and 2. The training dataset was used for the success rate and the spatial validation dataset for the prediction rate. The results were plotted in the ROC space along with the ROC plots (Fig. 6). The ROC curves reveal similar success and predictive capabilities for all susceptibility models, only the model 2 shows a value slightly lower.

The distance to perfect classification (r) was obtained for every model with the TPR and FPR values.

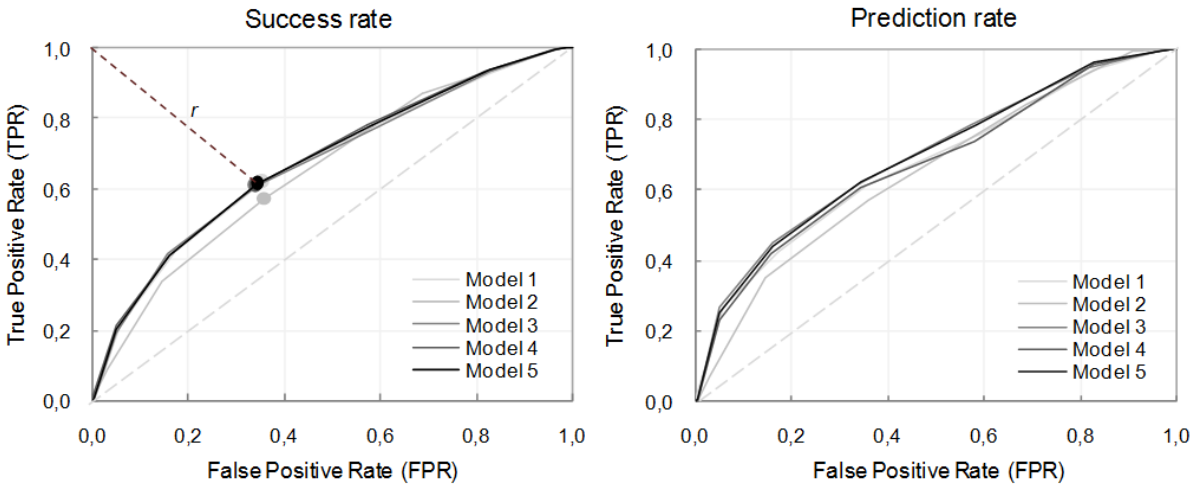

Fig. 6 Distance to perfect classification (r) and ROC success and prediction rate curves for each model. The dotted line shows the shortest r-value, which corresponds to M5.

In Table 2 are defined the statistic used in this study. The AUROC-values for all the models indicate an acceptable ability to distinguish between susceptible and non-susceptible areas. The hit rate, also referred as sensitivity or positive accuracy, expresses the proportion of positive cases correctly predicted. The False Alarm Rate, also called negative error, is the ratio between false positive and the total actual negatives. The odds ratio makes use of all the values in the confusion matrix because shows the ratio between correctly and incorrectly classified observations.

Table 2 Results of the different validation methods. Model AUC ROC values for the success and prediction rate, distance to perfect classification (r), and ROC metrics hit rate and false alarm rate.

Models	AUC ROC success rate (%)	AUC Prediction rate (%)	Distance to perfect classification (r)	Hit rate (TPR) (%)	False alarm rate (FPR) (%)	Odds ratio (OR)
M1	68,1	67,3	0,521	0,619	0,356	2,94
M2	65,0	64,9	0,574	0,554	0,361	2,19
M3	68,2	67,3	0,518	0,611	0,342	3,02
M4	68,8	69,5	0,520	0,606	0,339	2,99
M5	68,7	69,4	0,517	0,613	0,343	3,03

According to the results obtained both M4 and M5 have a good and similar trend as the success and prediction rate. M4 is slightly better on ROC plot (68,8% AUC) against 68,7% of the M5. However M5 shows a lower distance to perfect classification (0,517), and a slightly higher values in hit rate, false alarm rate, and the frequency distribution curves (Fig. 5). Hence, it is observed that using three factors give higher accuracy than that of using all the five factors.

Table 3 shows the LR coefficients of the susceptibility model M5 that correlate each factor to landslide occurrence (Table 3). LR gives a coefficient for every non-categorical variable and a coefficient for every class of the categorical variables.

Table 3 Coefficient values of logistic regression for each model.

Model	Factor	Class	Pixel percentage (%)	Percentage of pixels showing landslide occurrence (%)	Coefficient of logistic regression
M5	Aspect (AS)	0-360 degree	100	100	0,004
	Land cover	Agricultural land (AL)	20,8	8,6	-0,226
		Bare land (BL)	0,7	0,3	0,933
		Forest (F)	54,8	66,3	0,000
		Grassland (GL)	22,7	24,8	0,456
		Urban area (UA)	0,7	0	-20,141
		Water body (WB)	0,3	0	-19,306
	Slope (SL)	0-78,5 degree	100	100	0,040
	Intercept				-2,075

The probability of landslide occurrence was calculated applying Eq. 1 and Eq. 2, which use the LR coefficient data in Table 3 and each variable raster. Then, it was necessary to produce a binary raster for every class of the categorical variables, in which 1 was the presence of the class (i.e. grassland) and 0 any other values.

Eq. 8 shows how Eq. 2 was formulated to the model M5.

$$z = (-2{,}075) + (0{,}004 \times AS) + (-0{,}226 \times AL) + (0{,}933 \times BL) + (0{,}456 \times GL) + (-20{,}141 \times UA) + (-19{,}306 \times WB) + (0{,}040 \times SL) \quad (8)$$

After building the model and obtained by equation 2 a continuous response variable expressing the degree of susceptibility a decision threshold (cutoff value) of P(y) = 50% was selected to divide the continuous response depend variable into landslide or non.-landslide. This value corresponds to the same inflexion point of the ROC plot and the point to the distance to the perfect classification. The confusion matrix was performed by comparing this prediction with the observations in the validation landslide inventory dataset. The results, presented in Table 4, shows the number of correctly and incorrectly predicted observations, for both positive and negatives cases. The false positives, or error type I, corresponds to 34.3 %; on the other hand, 38,7 % represent the false negatives, or error type II.

Table 4 Confusion matrix for M5; inventory positives are cells with landslides, negatives otherwise. These values are compared with P(y) (probability estimated by LR). Total correct and incorrect predicted cells are shown on the right.

Model probability		Inventory positives		Inventory negatives			Total	
		n	%	n	%		n	%
M5								
P(y)>50%	Yes	**511**	**61.3**	127914	34.3	**Correct**	**245299**	**65.7**
P(y)<50%	No	323	38.7	**244788**	**65.7**	Incorrect	128237	34.3
Total (Σ)		834	100.0	372702	100.0		373691	100.0

Figure 7 shows the main graphical output and results obtained thought the validation phase for M5 model. It includes ROC plot success and prediction rates with the AUC value, and a fourfold representation of the confusion matrix. The susceptibility map is presented in Figure 8. The probability histogram was divided into the three susceptibility classes (Table 5). The upper limit of the medium class is the inflexion point of the ROC curve that is the same point of the distance to the perfect classification (0,5). And the lower limit of the medium class is a subtle change of slope there is in 0,3 value.

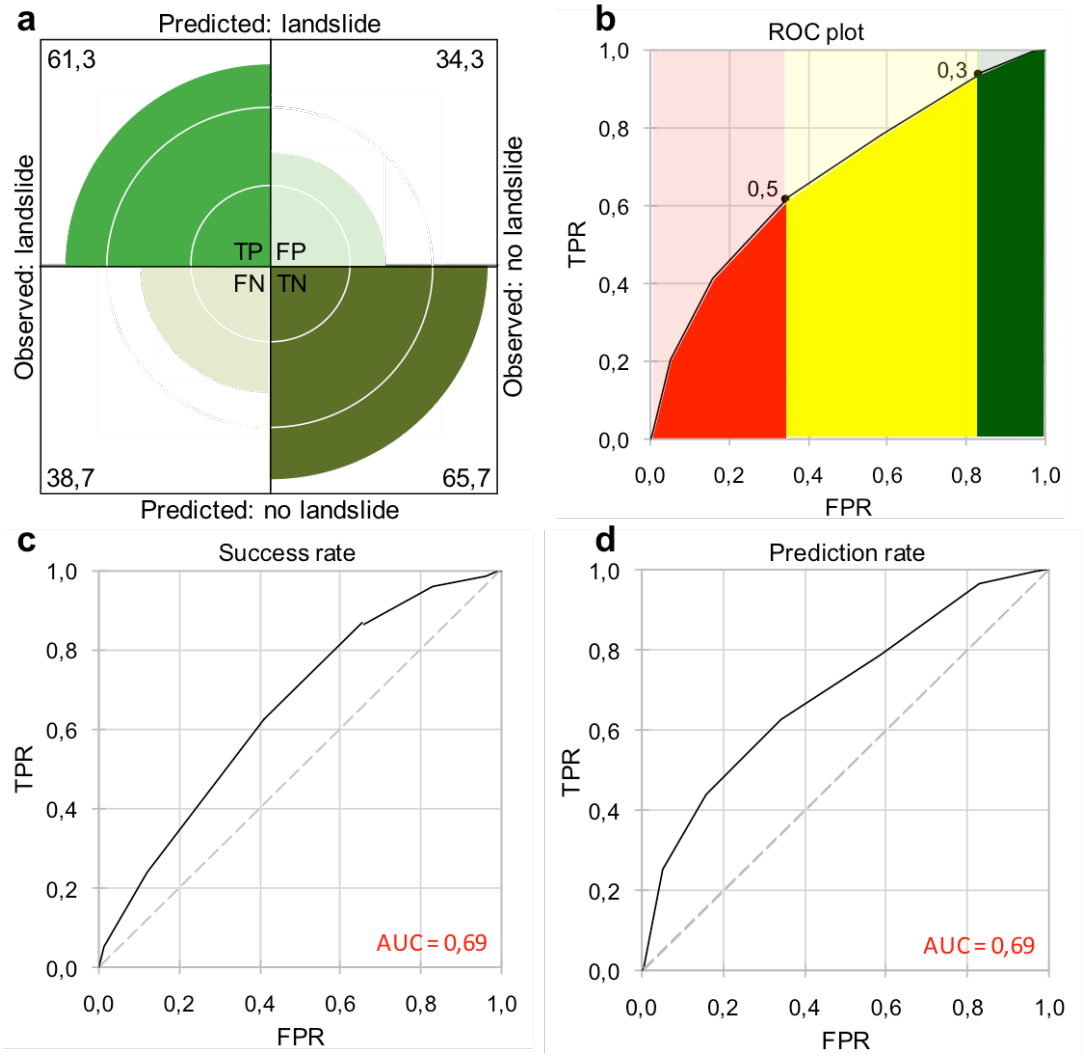

Fig. 7 Graphical output summary for model M5. (a) Fourfold plot summarizing the percentage value of true positives (TP), true negatives (TN), false positives (FP), and false negatives (FN); (b) landslide susceptibility classes classification; (c) ROC curve; (d) prediction rate curve.

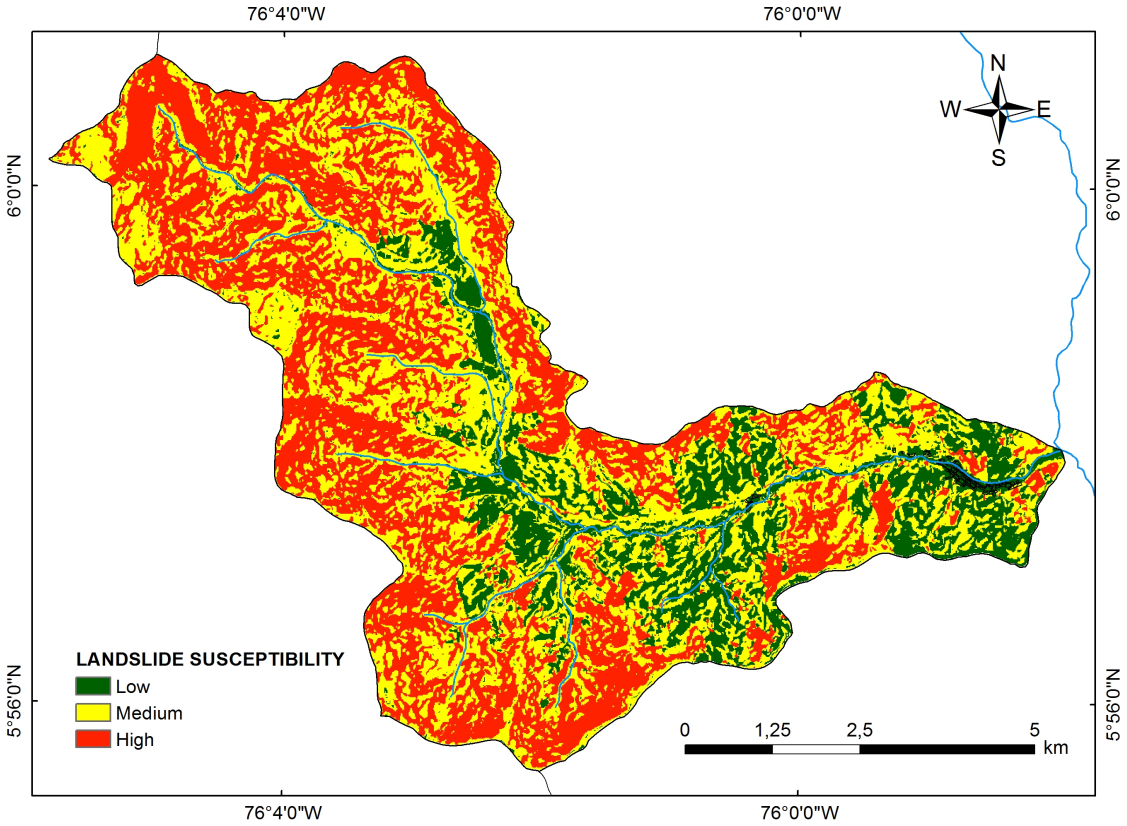

Fig. 8 Landslide susceptibility map for the study area produced by logistic regression and M5 variable combination (aspect, land cover and slope).

According to the landslide susceptibility map acquired from LR (Fig. 8), 34,4% (20,1 km^2) of the entire area was classified as being highly susceptible, while about 48,4% (28,3 km^2) was found to be on medium landslide susceptibility zones. Low susceptible zones showed 17,2% (10,0 km^2) of the entire area.

High susceptibility zones have a landslide density of 25,7 landslides/km^2, while 64,7% of the landslides triggered on May 18th, 2015 were on this susceptibility class. On medium susceptibility zones, 35,3% of May 18th, 2015 occurred. And on low susceptibility zones there are 4,9 landslides/km^2 and none of them is associated with May 18th, 2015 event.

Table 5 Landslide susceptibility classes description.

Probability range	Susceptibility class name	Area covered (km^2)	Area covered (%)	Landslide area (m^2)	Landslide area (%)	Landslide density (landslides/km^2)
0,0-0,3	Low	10,0	17,2	7056	5,8	4,9
0,3-0,5	Medium	28,3	48,4	42656	32,6	9,7
0,5-1,0	High	20,1	34,4	80625	61,6	25,7

Temporal validation with the event of May 18th, 2015

The landslide susceptibility map is validated using the landslide inventory of the event occurred on May 18, 2015. A comparison of the susceptibility map and event-based landslide inventory was carried out in an area of 8,6 km^2, 14,7% of the total area of study, which corresponds to the upper zone of the basin in which all the MORLE-type landslide event occurred. For this area the prediction rate was calculated with an AUC value of 0,55. The degree of fit of the three susceptibility are shown in Figure 9. Both show a relation between landslide occurrence of the May 18, 2017 event and high susceptibility areas.

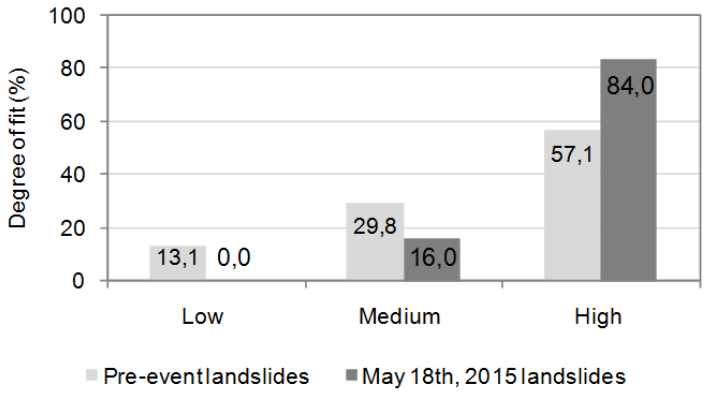

Fig. 9 Degree of fit of susceptibility classes.

6 Discussion

Landslide susceptibility mapping in tropical mountainous areas is usually difficult because of complex terrains, dense vegetation, weather conditions, and data scarcity. A huge region of the Colombian complex and tropical Andes terrains show these conditions, where landslide disasters are very common. This is the case of the La Liboriana catchment and Salgar disaster in May 18th, 2015.

Free and open remote sensing tools, such as Google Earth and Alaska Satellite Facility program, could be used to landslide susceptibility assessment in scarce-data zones. They are not only useful for the elaboration of the inventory map, but to obtain morphometric factors associated to landslide occurrence or to complete the missing data of environmental causative factors, such as land cover. They can be supported and complemented by traditional tools like aerial photography and satellite imagery.

Based on availability and accessibility of information the causative factors used for the analysis correspond to the most common predictor variables for landslide occurrence: aspect, land use,

curvature, slope gradient and TWI. Many other DEM derived variables can be obtained and could be included into the analysis, however correlation among variables increase reducing the prediction capacity of the model. Several studies have demonstrated there is no a number or standard landslide causative factors (Lee et al., 2008). In this study the spatial validation process using the multitemporal landslide inventory was used to select the most effective causative factors for La Liboriana catchment: aspect, land cover and slope gradient. Curvature and TWI were considered to be less effective factors, since both were not included in the final model.

However the most effective variables vary from one case study to another, so it should be always a matter of study which ones to include in the models. Lithology, which was relevant in different case studies (Atkinson & Massari, 1998; Ayalew & Yamagishi, 2005; Kavzoglu et al., 2015; Shahabi & Hashim, 2015) turned out to be absolutely irrelevant and it is excluded from the analysis. The results indicate that a large number of causative factors does not necessarily produce a better landslide susceptibility assessment. It could be associated to a high correlation between factors or a low correlation between the factors and the landslide occurrence.

Although the simulations carried out in this study did not incorporate local lithology or field mapping variables, the results show good success and prediction rates for unstable sites in tropical mountainous terrain. This suggests that landslide susceptibility in such environments are driven by topographic, DEM-derived variables. This also indicates that using free access tools to obtain data, a GIS-based analysis and multivariate statistical methods it is possible to simulate landslide susceptibility.

Although the success and prediction rate obtained for the model using the pre-event landslide inventory provide satisfactory results, the prediction rate of the model for the May 18th, 2015 event was just over the random prediction (AUC=0,55). The lower prediction rate is inferred to be a result to the accuracy of the landslide inventory map, related especially to the completeness of the map. Guzzetti et al (2012) defines the completeness of a landslide inventory map as the proportion of landslides shown in the inventory compared to the real number of landslides in the study area. It is related to the size of the landslides. Landslide scarps associated to small and shallow landslides, such as the May 15th, 2015 event, do not conserve discernible morphological signs. This type of scars and deposits are difficult to identify in tropical environments because weathering and vegetation cover or erase any physical evidence. The vegetation growth in the area is accelerated because it is a tropical forest area, and there are great morphological changes that make it difficult to identify them through photo-interpretation and other remote sensing tools. The distribution of the past landslides that was used in the calibration process is not adequate to predict landslides such as

the event on May 18th, 2015. Having some inventoried that may have occurred previously to May 18th, 2015 could improve the prediction capability of the model. The pre-event landslides incorporated into the landslide inventory correspond to recent or depth-seated landslides.

Considering this scenario, the LR method was also applied using the whole landslide inventory (pre-event landslides and May 18th, 2015 landslides included). The cross validation in this case was made splitting the data into two groups of 75% and 25%, for training and validation each one. The ROC analysis success rate obtained was 0,65 and the prediction rate of 0,67 (Fig 10). The results show the final success and prediction rate does not improve, indicating that multitemporal landslide inventory are more suitable to train and calibrate landslide susceptibility assessment models, and MORLE type events should be used carefully.

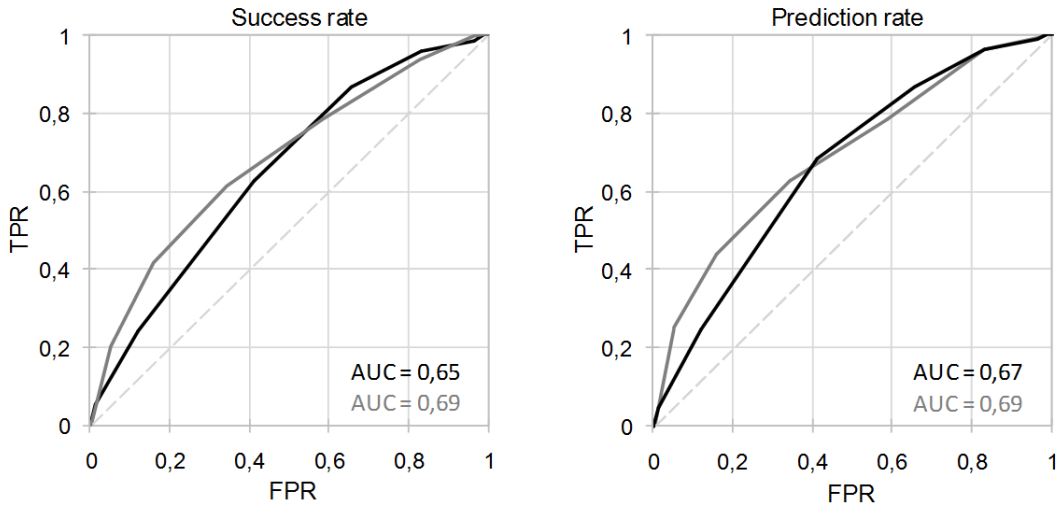

Fig. 10 ROC plot and prediction rate curves comparison for the models. May 18th, 2015 and pre-event landslides included (black); only pre-event landslides included (grey).

Another important outcome of this work is the …

The expansion of settlements in interandean valleys during the last century contributed to increase the risk for human lives and infrastructures. To identify the risk caused by debris and flash floods to human settlements, it is of primary importance to detect the areas susceptible to landslide occurrence.

False positives can be either certainly error in the model, or else real susceptibility-prone areas that have not yet developed landslides.

7 Conclusions

In this work, we propose a very helpful approach to assess landslide susceptibility to be used in similar zones worldwide; which may also have data scarcity due to difficult conditions and accessibility. Data availability is a challenge for many researchers especially in developing countries where many catchments remain remote and difficult to access. The La Liboriana catchment is a tropical and complex terrain region that is affected periodically by landslides triggered by rainfall, but it lacks essential data for landslide susceptibility and hazard analysis. The porpose approach is based on freely available DEM data and Google Earth image satellite to provide landslide inventory and predictors variables. The data obtained was used as input for a multivariate statistical logistic regression analysis. The results obtained show that the aim of this work has been essentially achieved.

It is important to continue studying past landslides triggered by rainstorm in forested areas, because in most of the cases they caused a major disaster. It may help to develop early warning systems for the community, and reduce economical and human annual losses.

References

Aleotti, P., & Chowdhury, R. (1999). Landslide hazard assessment: summary review and new perspectives. *Bulletin of Engineering Geology and the Environment*, *58*(1), 21–44. http://doi.org/10.1007/s100640050066

Alexander, D. (2005). Vulnerability to Landslides. In T. Glade, M. Anderson, & M. J. Crozier (Eds.), *Landslide Hazard and Risk* (pp. 175–198). John Wiley & Sons, Ltd. http://doi.org/10.1002/9780470012659.ch5

ASF-DAAC. (2015). ALOS-1 PALSAR_Radiometric_Terrain_Corrected_low_res; JAXA/METI, 2007. En la página web del Alaska Satellite Facility ASF DAAC. http://doi.org/10.5067/JBYK3J6HFSVF

Atkinson, P. M., & Massari, R. (1998). Generalised linear modelling of susceptibility to landsliding in the Central Apennines, Italy. *Computers & Geosciences*, *24*(4), 373–385. http://doi.org/10.1016/S0098-3004(97)00117-9

Ayalew, L., & Yamagishi, H. (2002). Landslides in the Kakuda-Yahiko Mountains of Niigata, Their Analyses and Description Using GIS. *National Congress of Engineering Geological Society of Japan, Takamatsu, Japan*, 131–134.

Ayalew, L., & Yamagishi, H. (2005). The application of GIS-based logistic regression for landslide susceptibility mapping in the Kakuda-Yahiko Mountains, Central Japan. *Geomorphology*, *65*(1–2), 15–31. http://doi.org/10.1016/j.geomorph.2004.06.010

Ayalew, L., Yamagishi, H., Marui, H., & Kanno, T. (2005). Landslides in Sado Island of Japan: Part II. GIS-based susceptibility mapping with comparisons of results from two methods and verifications. *Engineering Geology*, *81*(4), 432–445. http://doi.org/10.1016/j.enggeo.2005.08.004

Bai, S. B., Wang, J., Lü, G. N., Zhou, P. G., Hou, S. S., & Xu, S. N. (2010). GIS-based logistic regression for landslide susceptibility mapping of the Zhongxian segment in the Three Gorges

area, China. *Geomorphology*, *115*(1–2), 23–31. http://doi.org/10.1016/j.geomorph.2009.09.025

Baum, R. L., Savage, W. Z., & Godt, J. W. (2008). TRIGRS — A Fortran Program for Transient Rainfall Infiltration and Grid-Based Regional Slope-Stability Analysis, Version 2.0. *U.S. Geological Survey Open-File Report*, (2008–1159), 75. http://doi.org/Open-File Report 2008–1159

Brenning, A. (2005). Spatial prediction models for landslide hazards: review, comparison and evaluation. *Natural Hazards and Earth System Sciences*, *5*, 853–862. http://doi.org/10.5194/nhess-5-853-2005

Calle, B., González, H., de la Peña, R., Escorce, E., & Durango, J. (1980). Geología de la Plancha 166 Jericó. Bogotá: INGEOMINAS.

Calle, B., & Salinas, R. (1984). Geología de la Plancha 165 Carmen de Atrato. Bogotá: INGEOMINAS.

Cardinali, M., Reichenbach, P., Guzzetti, F., Ardizzone, F., Antonini, G., Galli, M., … Salvati, P. (2002). A geomorphological approach to the estimation of landslide hazards and risks in Umbria, Central Italy. *Natural Hazards and Earth System Sciences*, *2*(1–2), 57–72. http://doi.org/10.5194/nhess-2-57-2002

Carrara, A. (1983). Multivariate Models for Landslide Hazard Evaluation. *Mathematical Geology*, *15*(3), 403–426.

Cepeda, J., Chávez, J. A., & Cruz Martínez, C. (2010). Procedure for the selection of runout model parameters from landslide back-analyses: application to the Metropolitan Area of San Salvador, El Salvador. *Landslides*, *7*(2), 105–116. http://doi.org/10.1007/s10346-010-0197-9

Chacón, J., Irigaray, C., Fernández, T., & El Hamdouni, R. (2006). Engineering geology maps: Landslides and geographical information systems. *Bulletin of Engineering Geology and the Environment*, *65*(4), 341–411. http://doi.org/10.1007/s10064-006-0064-z

Chevalier, G. G., Medina, V., Hürlimann, M., & Bateman, A. (2013). Debris-flow susceptibility analysis using fluvio-morphological parameters and data mining: application to the Central-Eastern Pyrenees. *Natural Hazards*, *67*(2), 213–238. http://doi.org/10.1007/s11069-013-0568-3

Chung, C.-J. F., & Fabbri, A. G. (2003). Validation of Spatial Prediction Models for Landslide Hazard Mapping. *Natural Hazards*, *30*, 451–472. http://doi.org/10.1023/B

Clerici, A., Perego, S., Tellini, C., & Vescovi, P. (2002). A procedure for landslide susceptibility zonation by the conditional analysis method. *Geomorphology*, *48*(4), 349–364. http://doi.org/http://dx.doi.org/10.1016/S0169-555X(02)00079-X

Costanzo, D., Rotigliano, E., Irigaray, C., Jiménez-Perálvarez, J. D., & Chacón, J. (2012). Factors selection in landslide susceptibility modelling on large scale following the gis matrix method: application to the river Beiro basin (Spain). *Nat. Hazards Earth Syst. Sci.*, *12*(2), 327–340. http://doi.org/10.5194/nhess-12-327-2012

Crozier, M. J. (2005). Multiple-occurrence regional landslide events in New Zealand: Hazard management issues. *Landslides*, *2*(4), 247–256. http://doi.org/10.1007/s10346-005-0019-7

Cruz Roja Colombiana. (2017). Emergencia Mocoa-Putumayo: reporte de situación #13. *Reporte de Situación*, (13), 1–17. Retrieved from http://www.cruzrojacolombiana.org/noticias-y-prensa/reportes-de-situación-emergencia-mocoa

De Graff, J. V, Romesburg, H. C., Ahmad, R., & McCalpin, J. P. (2012). Producing landslide-susceptibility maps for regional planning in data-scarce regions. *Natural Hazards*, *64*(1), 729–749. http://doi.org/10.1007/s11069-012-0267-5

Dilley, M., Chen, R. S., Deichmann, U., Lerner-Lam, A. L., & Arnold, M. (2005). *Natural Disaster Hotspots A Global Risk Analysis*. *Earth Science* (Vol. 98). Washington, DC: The World Bank, Hazard Management Unit. http://doi.org/10.1080/01944360902967228

Donati, L., & Turrini, M. C. (2002). An objective method to rank the importance of the factors predisposing to landslides with the GIS methodology: application to an area of the Apennines

(Valnerina; Perugia, Italy). *Engineering Geology*, *63*(3–4), 277–289. http://doi.org/http://dx.doi.org/10.1016/S0013-7952(01)00087-4
Ermini, L., Catani, F., & Casagli, N. (2005). Artificial Neural Networks applied to landslide susceptibility assessment. *Geomorphology*, *66*(1–4 SPEC. ISS.), 327–343. http://doi.org/10.1016/j.geomorph.2004.09.025
Fawcett, T. (2006). An introduction to ROC analysis. *Pattern Recognition Letters*, *27*(8), 861–874. http://doi.org/10.1016/j.patrec.2005.10.010
Fell, R., Corominas, J., Bonnard, C., Cascini, L., Leroi, E., & Savage, W. Z. (2008). Guidelines for landslide susceptibility, hazard and risk zoning for land-use planning. *Engineering Geology*, *102*(3–4), 99–111. http://doi.org/10.1016/j.enggeo.2008.03.014
Fernández, T., Irigaray, C., El Hamdouni, R., & Chacón, J. (2003). Methodology for landslide susceptibility mapping by means of a GIS. Application to the contraviesa area (Granada, Spain). *Natural Hazards*, *30*(3), 297–308. http://doi.org/10.1023/B:NHAZ.0000007092.51910.3f
Galli, M., Ardizzone, F., Cardinali, M., Guzzetti, F., & Reichenbach, P. (2008). Comparing landslide inventory maps. *Geomorphology*, *94*(3–4), 268–289. http://doi.org/10.1016/j.geomorph.2006.09.023
Garcia, M. (1988). Eventos catastroficos del 13 de Noviembre de 1985. *Boletin de Vias*, *15*(65), 7–106.
Gorsevski, P.V.; Gessler, P.;Foltz, R. B. (2000). Spatial Prediction of Landslide Hazard Using Discriminant Analysis and GIS. *4th International Conference on Integrating GIS and Environmental Modeling (GIS/EM4); Problems, Prospects and Research Needs*.
Greco, R., Sorriso-Valvo, M., & Catalano, E. (2007). Logistic Regression analysis in the evaluation of mass movements susceptibility: The Aspromonte case study, Calabria, Italy. *Engineering Geology*, *89*(1–2), 47–66. http://doi.org/10.1016/j.enggeo.2006.09.006
Guha-Sapir, D., Hoyois, P., & Below, R. (2016). Annual Disaster Statistical Review 2015: The numbers and trends. *CRED*, 1–59. http://doi.org/10.1093/rof/rfs003
Guzzetti, F., Carrara, A., Cardinali, M., & Reichenbach, P. (1999). Landslide hazard evaluation: A review of current techniques and their application in a multi-scale study, Central Italy. *Geomorphology*, *31*(1–4), 181–216. http://doi.org/10.1016/S0169-555X(99)00078-1
Guzzetti, F., Mondini, A. C., Cardinali, M., Fiorucci, F., Santangelo, M., & Chang, K. T. (2012). Landslide inventory maps: New tools for an old problem. *Earth-Science Reviews*, *112*(1–2), 42–66. http://doi.org/10.1016/j.earscirev.2012.02.001
Guzzetti, F., Peruccacci, S., Rossi, M., & Stark, C. P. (2007). Rainfall thresholds for the initiation of landslides in central and southern Europe. *Meteorology and Atmospheric Physics*, *98*(3), 239–267. http://doi.org/10.1007/s00703-007-0262-7
Hussin, H. Y., Zumpano, V., Reichenbach, P., Sterlacchini, S., Micu, M., van Westen, C., & Bălteanu, D. (2016). Different landslide sampling strategies in a grid-based bi-variate statistical susceptibility model. *Geomorphology*, *253*, 508–523. http://doi.org/10.1016/j.geomorph.2015.10.030
Iverson, R. M. (2000). Landslide triggering by rain infiltration. *Water Resources Research*, *36*(7), 1897. http://doi.org/10.1029/2000WR900090
Kavzoglu, T., Kutlug Sahin, E., & Colkesen, I. (2015). Selecting optimal conditioning factors in shallow translational landslide susceptibility mapping using genetic algorithm. *Engineering Geology*, *192*, 101–112. http://doi.org/10.1016/j.enggeo.2015.04.004
Lee, S. (2005). Application of logistic regression model and its validation for landslide susceptibility mapping using GIS and remote sensing data. *International Journal of Remote Sensing*, *26*(December), 1477–1491. http://doi.org/10.1080/01431160412331331012
Lee, S., & Pradhan, B. (2007). Landslide hazard mapping at Selangor, Malaysia using frequency ratio and logistic regression models. *Landslides*, *4*(1), 33–41. http://doi.org/10.1007/s10346-006-0047-y

Lee, S., Ryu, J., Won, J., & Park, H. (2004). Determination and application of the weights for landslide susceptibility mapping using an artificial neural network. *Engeneering Geology*, *71*(April 2016), 289–302. http://doi.org/10.1016/S0013-7952(03)00142-X

Lee, S., & Talib, J. A. (2005). Probabilistic landslide susceptibility and factor effect analysis. *Environmental Geology*, *47*(7), 982–990. http://doi.org/10.1007/s00254-005-1228-z

Lin, C. W., Tseng, C. M., Tseng, Y. H., Fei, L. Y., Hsieh, Y. C., & Tarolli, P. (2013). Recognition of large scale deep-seated landslides in forest areas of Taiwan using high resolution topography. *Journal of Asian Earth Sciences*, *62*, 389–400. http://doi.org/10.1016/j.jseaes.2012.10.022

Mileti, D. S., Bolton, P. A., Fernandez, G., & Updike, R. G. (1991). *The Eruption of Nevado Del Ruiz Volcano Colombia, South America, November 13, 1985*. Washington, DC: National Research Council. The National Academies Press. http://doi.org/10.17226/1784

Montgomery, D. R., & Dietrich, W. E. (1994). A physically based model for the topographic control on shallow landsliding. *Water Resources Research*, *30*(4), 1153–1171. http://doi.org/10.1029/93WR02979

Moore, I. D., Grayson, R. B., & Ladson, A. R. (1991). Digital terrain modelling: A review of hydrological, geomorphological, and biological applications. *Hydrological Processes*, *5*(1), 3–30. http://doi.org/10.1002/hyp.3360050103

Nadim, F., Kjekstad, O., Peduzzi, P., Herold, C., & Jaedicke, C. (2006). Global landslide and avalanche hotspots. *Landslides*, *3*(2), 159–173. http://doi.org/10.1007/s10346-006-0036-1

Pack, R. T. (1998). The SINMAP Approach to Terrain Stability Mapping. *8th Congress of the International Association of Engineering Geology*, 8.

Pawluszek, K., & Borkowski, A. (2016). Impact of DEM-derived factors and analytical hierarchy process on landslide susceptibility mapping in the region of Rożnów Lake, Poland. *Natural Hazards*, *86*(2), 919–952. http://doi.org/10.1007/s11069-016-2725-y

Petley, D. (2008). The global occurrence of fatal landslides in 2007. In *International Conference on Management of Landslide Hazard in the Asia–Pacific Region. Japan Landslide Society, Tokyo Japan.* (pp. 590–600). Tokyo, Japan.

Petley, D. (2012). Global patterns of loss of life from landslides. *Geology*, *40*(10), 927–930. http://doi.org/10.1130/G33217.1

Poli, S., & Sterlacchini, S. (2007). Landslide representation strategies in susceptibility studies using weights-of-evidence modeling technique. *Natural Resources Research*, *16*(2), 121–134. http://doi.org/10.1007/s11053-007-9043-8

Pourghasemi, H. R., Mohammady, M., & Pradhan, B. (2012). Landslide susceptibility mapping using index of entropy and conditional probability models in GIS: Safarood Basin, Iran. *Catena*, *97*(October), 71–84. http://doi.org/10.1016/j.catena.2012.05.005

Poveda, G. (2004). La Hidroclimatología De Colombia : Una Síntesis Desde La Escala Inter-Decadal Hasta La Escala Diurna. *Revista de La Academia Colombiana de Ciencias*, *28*(107), 201–222.

Poveda, G., Mesa, O. J., Salazar, L. F., Arias, P. a., Moreno, H. a., Vieira, S. C., … Alvarez, J. F. (2005). The Diurnal Cycle of Precipitation in the Tropical Andes of Colombia. *Monthly Weather Review*, *133*(1), 228–240. http://doi.org/10.1175/MWR-2853.1

Pradhan, B., & Lee, S. (2010). Landslide susceptibility assessment and factor effect analysis: backpropagation artificial neural networks and their comparison with frequency ratio and bivariate logistic regression modelling. *Environmental Modelling and Software*, *25*(6), 747–759. http://doi.org/10.1016/j.envsoft.2009.10.016

Schuster, R. (1996). Socioeconomic significance of landslides. In A. K. Turner & R. L. Schuster (Eds.), *Landslides: Analysis and control* (pp. 12–35). Washington, DC: National Res. Council, Transp. Res. Board Spec. Report 247.

Schuster, R., & Fleming, R. W. (1986). Economic losses and fatalities due to landslides. *Bulletin of the Association of Engineering Geologists*, *23*(1), 11–28. Retrieved from

http://pubs.er.usgs.gov/publication/70015022
Schuster, R., & Highland, L. M. (2001). *Socioeconomic effects of landslides in Western Hemisphere*. Retrieved from https://pubs.usgs.gov/of/2001/ofr-01-0276/
Schuster, R., Salcedo, D. A., & Valenzuela, L. (2002). Overview of catastrophic landslides of South America in the twentieth century. In S. G. Evans & J. V. de Graff (Eds.), *Catastrophic landslides: effects, occurrences, mechanisms.* (pp. 1–34). Geological Society of America Reviews in Engineering Geology XV.
Sepúlveda, S. A., & Petley, D. N. (2015). Regional trends and controlling factors of fatal landslides in Latin America and the Caribbean. *Natural Hazards and Earth System Sciences*, *15*(8), 1821–1833. http://doi.org/10.5194/nhess-15-1821-2015
Shahabi, H., & Hashim, M. (2015). Landslide susceptibility mapping using GIS-based statistical models and Remote sensing data in tropical environment. *Scientific Reports*, *5*, 9899. http://doi.org/10.1038/srep09899
Simon, N., Crozier, M., de Roiste, M., & Rafek, A. G. (2013). Point based assessment: Selecting the best way to represent landslide polygon as point frequency in landslide investigation. *Electronic Journal of Geotechnical Engineering*, *18*(Bund. D), 775–784.
Soeters, R., & van Westen, C. J. (1996). Slope instability recognition,analysis and zonation, In: Turner, A.K., Schuster, R.L., Eds., Landslides: Investigation and Mitigation: TRB Sp. Rep. 247. *National Research Council, National Academy Press, Washington DC*, 129–177.
Süzen, M. L., & Doyuran, V. (2004). Data driven bivariate landslide susceptibility assessment using geographical information systems: A method and application to Asarsuyu catchment, Turkey. *Engineering Geology*, *71*(3–4), 303–321. http://doi.org/10.1016/S0013-7952(03)00143-1
Tazik, E., Jahantab, Z., Bakhtiari, M., Rezaei, A., & Alavipanah, S. K. (2014). Landslide susceptibility mapping by combining the three methods Fuzzy Logic, frequency ratio and Analytical Hierarchy Process in Dozain basin. *International Archives of the Photogrammetry, Remote Sensing and Spatial Information Sciences - ISPRS Archives*, *40*(2W3), 267–272. http://doi.org/10.5194/isprsarchives-XL-2-W3-267-2014
Thiery, Y., Malet, J. P., Sterlacchini, S., Puissant, A., & Maquaire, O. (2007). Landslide susceptibility assessment by bivariate methods at large scales: Application to a complex mountainous environment. *Geomorphology*, *92*(1–2), 38–59. http://doi.org/10.1016/j.geomorph.2007.02.020
Tokuhiro, H. (1999). Landslide in Villa Tina, Medellin City, Colombia. In K. Sassa (Ed.), *Landslides of the world* (pp. 198–201). Japan Landslide Soc., Kyoto Univ. Press.
Van Den Eeckhaut, M., Vanwalleghem, T., Poesen, J., Govers, G., Verstraeten, G., & Vandekerckhove, L. (2006). Prediction of landslide susceptibility using rare events logistic regression: A case-study in the Flemish Ardennes (Belgium). *Geomorphology*, *76*(3–4), 392–410. http://doi.org/10.1016/j.geomorph.2005.12.003
van Westen, C. J., Soeters, R., & Sijmons, K. (2000). Digital geomorphological landslide hazard mapping of the Alpago area, Italy. *International Journal of Applied Earth Observation and Geoinformation*, *2*(1), 51–60. http://doi.org/10.1016/S0303-2434(00)85026-6
Varnes, D. (1981). Slope-Stability Problems of Circum-Pacific Region as Related to Mineral and Energy Resources. In M. T. Halbouty (Ed.), *Energy Resources of the Pacific Region* (12th ed., pp. 489–505). Am. Assoc. Pet. Geol. Studies in Geol.
Voight, B. (1990). The 1985 Nevado del Ruiz volcano catastrophe: anatomy and retrospection. *Journal of Volcanology and Geothermal Research*, *44*(3), 349–386. http://doi.org/http://dx.doi.org/10.1016/0377-0273(90)90027-D
Yilmaz, I. (2010). Comparison of landslide susceptibility mapping methodologies for Koyulhisar, Turkey: conditional probability, logistic regression, artificial neural networks, and support vector machine. *Environmental Earth Sciences*, *61*(4), 821–836. http://doi.org/10.1007/s12665-009-0394-9
Zêzere, J. L., Trigo, R. M., & Trigo, I. F. (2005). Shallow and deep landslides induced by rainfall in

the Lisbon region (Portugal): assessment of relationships with the North Atlantic Oscillation. *Natural Hazards and Earth System Science*, *5*(3), 331–344. http://doi.org/10.5194/nhess-5-331-2005